UCRL-ID-128536

Phase Retrieval for Adaptive Optics System Calibration

James M. Brase, Carmen J. Carrano, Bruce A. Macintosh, Scot S. Olivier, Jong R. An

August 1997

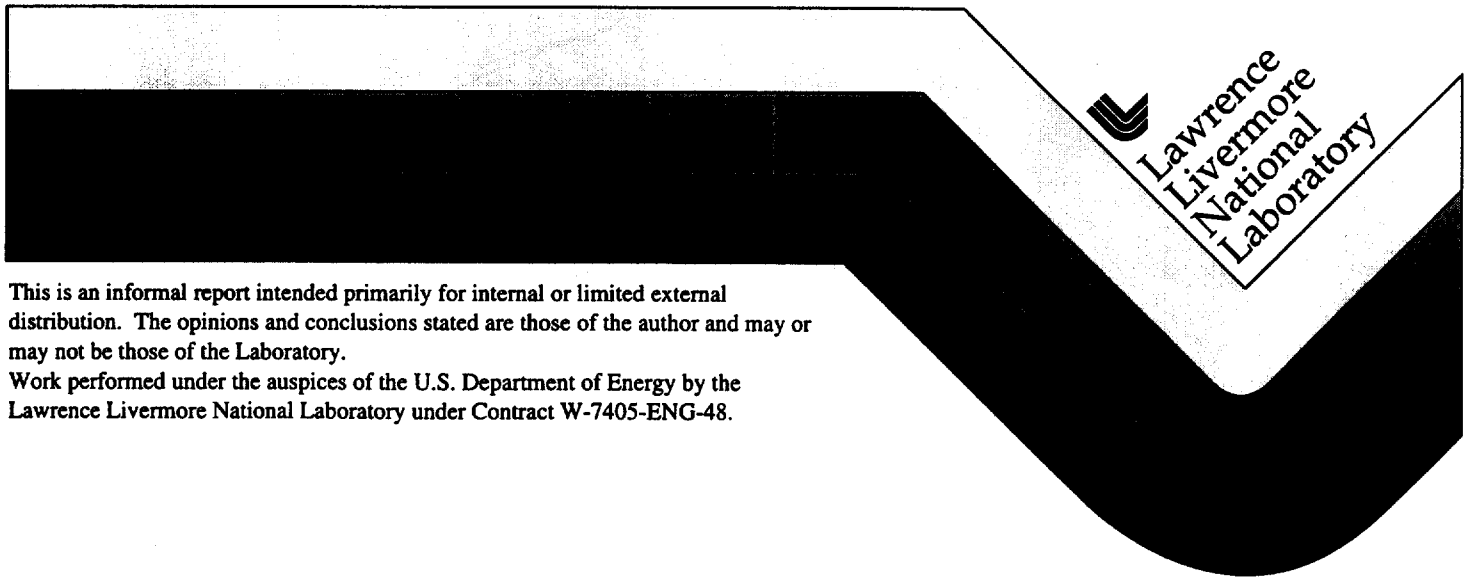

Work performed under the auspices of the U.S. Department of Energy by the Lawrence Livermore National Laboratory under Contract W-7405-ENG-48.

Phase Retrieval for Adaptive Optics System Calibration *

James M. Brase Carmen J. Carrano Bruce Macintosh Scot Olivier
Jong An

1 Introduction

Adaptive optics offers the possibility of correcting dynamic wavefront errors due to sources ranging from thermal aberrations in laser systems to atmospheric blurring in astronomical telescopes [1]. Advances in real-time control, sensors, and computation are making it possible to address challenging wavefront control problems at high levels of performance. The general wavefront correction approach is shown in Figure 1. An aberrated wavefront enters the system and is reflected from a correction element, most commonly a deformable mirror. The modified output wavefront is sampled and its wavefront measured; a typical approach is a Shack-Hartmann sensor which measures local tilt components. The measured output is compared to a reference which represents the desired output wavefront. The difference, the wavefront error, is used by a closed loop control system to modify the deformable mirror shape to drive the error to zero.

An important calibration in the use of an adaptive optics system is the determination of the reference wavefront. Usually, the objective is to make a diffraction limited image on the imaging sensor. Many AO systems, particularly those that use existing science instruments not specifically designed for AO-based observations, will have optical components after the wavefront sampling point. These optics are termed non-common-path optics in Figure 1 because any aberrations that they introduce cannot be measured by the wavefront sensor. Non-common-path wavefront errors will be transferred directly to the science image.

Our objective in this report is to develop methods to determine the output pupil wavefront using intensity measurements directly from the science detector. This wavefront can then be used to determine a reference wavefront which will precorrect for the non-common-path aberrations and produce the desired wavefront at the science detector. The general approach to this calibration method is

*Work performed under the auspices of the U.S. Department of Energy by the Lawrence Livermore National Laboratory under contract No. W-7405-ENG-48

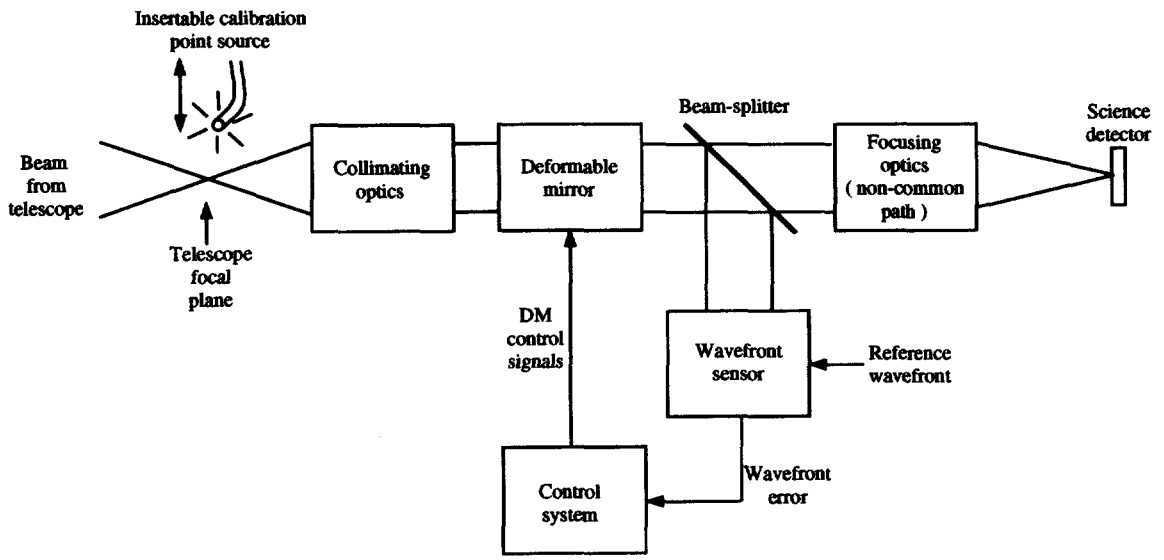

Figure 1: Block diagram of general wavefront correction approach for an adaptive optics system.

- Insert a point source at the system input, close the DM control loop, and set the reference to a flat wavefront; the image on the science detector represents the effects of non-common-path aberrations;
- Measure the output wavefront using phase retrieval from intensity images; the algorithms are described in detail in Section 2;
- Set the reference wavefront to the conjugate of the measured output wavefront; this should produce a flat wavefront at the science detector.

In this report we will describe two phase retrieval algorithms that can be used and a set of simulation studies of AO system calibration. We will present the initial experimental results of applying this technique in calibration of the Lick Observatory laser guidestar AO system in a later paper.

2 Phase retrieval approaches

There are a number of methods for performing phase retrieval presented in the literature, and they can be classified into two basic approaches. The first of these phase retrieval approaches uses a single intensity image measured at the focal plane of the optical system

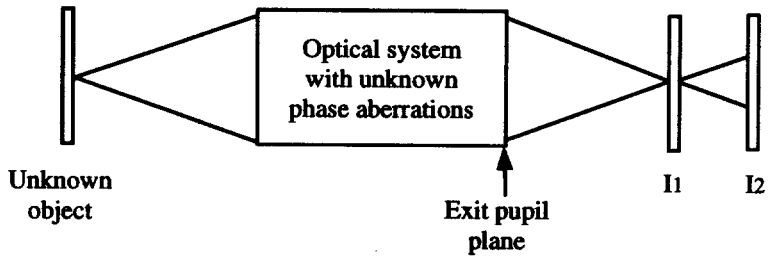

Figure 2: System diagram of phase retrieval concept. The intensity image at I_1 is taken in focus. If phase diversity is to be employed, a second intensity image at I_2 is recorded with a known defocus.

along with at least some knowledge of the pupil plane intensity distribution to estimate the aberrating wavefront [2] [4] [6]. The second phase retrieval approach incorporates phase diversity, which means that a second intensity image measured at a known defocus is also utilized in order to estimate not only the aberrating wavefront but the unknown object as well[3] [5] [7]. Figure 2 illustrates an optical system diagram for phase retrieval with and without phase diversity. The phase diversity approach has been used to correct the effects of atmospherically induced aberrations on systems which do not employ adaptive optics[8].

Even though for calibration of an adaptive optics system we are not necessarily interested in obtaining the unknown object, which would be a point source, both methodologies should provide us with an estimate of the aberrating wavefront. Therefore, we will investigate a common technique from each approach. We now give a brief explanation of each technique followed by simulation results which will be given in the next section.

The first phase retrieval technique we will investigate is commonly known as the Gerchberg-Saxton algorithm (GS) or the error-reduction algorithm [2] [4]. The iterative algorithm involves transforming back and forth between the pupil plane and the image plane and applying either measured data or known constraints at each plane. The intensity at the image plane is known because it is measured, but knowledge of the pupil plane is often limited to its region of support or aperture size. Of course, the more information you know about the pupil, such as if the intensity can be considered uniform over the aperture, the faster the algorithm will converge. A block diagram of the algorithm is depicted in Figure 3. Since the image plane data is measured at the focal point, it is possible to perform the propagation between planes using forward and inverse Fourier transforms.

The second phase retrieval technique we will investigate, which uses phase diversity, is a least-squares technique (LS) that leads to a maximum-likehood estimate for the phase aberrated wavefront [7]. Since we can describe the wavefront as a set of Zernike polynomials, we solve for the Zernike coefficents that minimize some error function. As with least squares

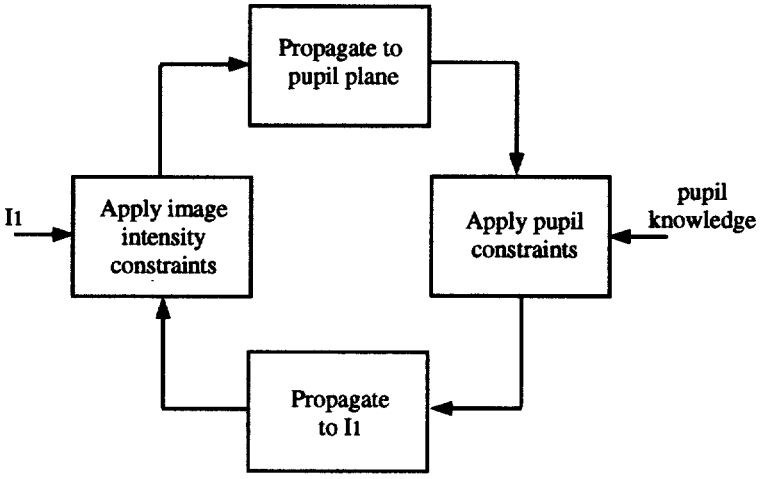

Figure 3: Block diagram of Gerchberg-Saxton error-reduction algorithm

techniques, the error function is the sum of the squared errors in the difference between the observed and estimated in and out of focus images. A simplified block diagram of the iterative procedure is shown in Figure 4 For a detailed explanation of this algorithm see reference [7].

3 Simulation results

For the phase retrieval simulations, it is necessary to define the optical system parameters as well as the known phase aberration that we will try to estimate. One useful way to describe a phase aberration is in terms of Zernike polynomials and coefficients, which makes the aberration straightforward to generate with the computer. The phase aberration that we will be using in the simulations is composed of several Zernike polynomials with coefficients given in Table 1; the phase image is shown in Figure 5.

In order to make the simulation more realistic we have added random noise to the intensity image measurement. Since the GS algorithm is iterative, the more iterations performed, the more accurate the results will be. A proof that the squared error can only decrease (or stay the same) is given in [4]. A plot of the mean squared error (MSE) between the estimated image magnitude at each iteration and the actual measured image magnitude is shown in Figure 6(a). In the plot, we can see that the MSE drops rapidly for the first ten iterations and then drops more slowly thereafter. In Figure 6(b) and (c) we also show the estimated phase aberrations after 50 and 100 iterations. If we perform a Zernike decomposition on each of the phase aberration estimates we can see quantitatively

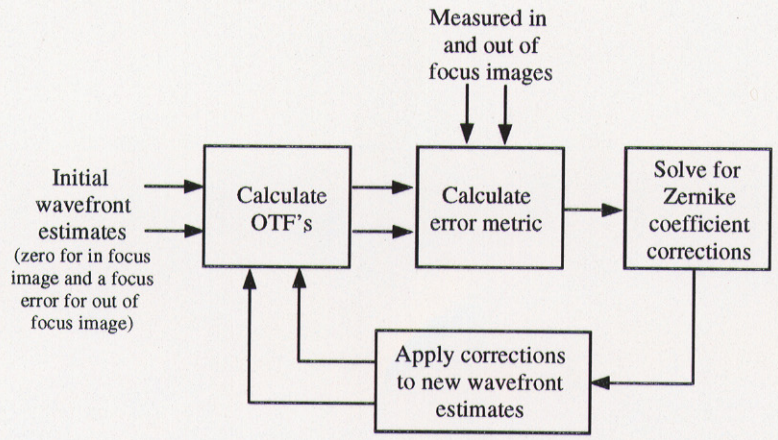

Figure 4: Block diagram of least squares phase diversity algorithm.

Zernike mode number	Coefficient
3	0.30
4	0.80
5	-0.20
7	0.50
11	0.10
all others	0

Table 1: Table of Zernike coefficients that compose the phase aberration

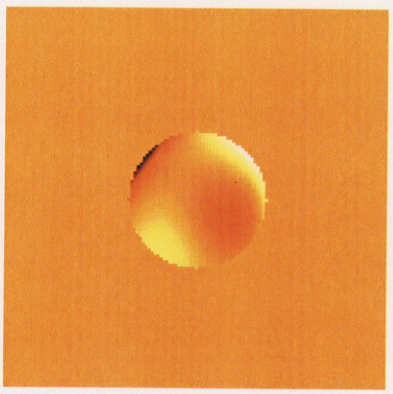

Figure 5: Image of the phase aberration used in the simulations. The image size is 128 pixels by 128 pixels. The aperture size is 46 pixels in diameter.

Zernike mode number	Actual Coefficient	50 Iterations	100 Iterations
3	0.30	0.054	0.28
4	0.80	0.66	0.79
5	-0.20	-0.32	-0.21
7	0.50	0.51	0.49
11	0.10	0.10	0.10
all others	0	$\leq$0.15	$\leq$0.015

Table 2: Table of Zernike coefficients estimated with the GS algorithm for 50 and 100 iterations compared with the actual coefficients.

Zernike mode number	Actual Coefficient	4 Iterations
3	0.30	0.30
4	0.80	0.80
5	-0.20	-0.20
7	0.50	0.50
11	0.10	0.10
all others	0	$\leq$0.0013

Table 3: Table of Zernike coefficients estimated with the LS algorithm after 4 iterations compared with the actual coefficients.

how the GS phase retrieval algorithm did for each case; the results are given in Table 2. From examining the Zernike coefficient values, we can see that 100 iterations gives a better estimate of the phase aberrations than 50 iterations does, mainly for the lower order modes.

Applying the LS algorithm requires an out of focus intensity (or phase diversity) image along with the in focus image. For the simulation, we use an image observation that is out of focus by one wave of focus(rms). For the LS algorithm, which is also iterative, convergence occurs much faster than for the GS algorithm, only four iterations on our simulated data. The resulting estimated phase aberration is displayed in Figure 7. Unlike the GS algorithm that estimates the phase aberration image directly, the LS aberration estimate is smooth because it estimates Zernike coefficients, which limit spatial frequency content. The estimated Zernike coefficients from the LS algorithm are listed in Table 3.

To fully and accurately compare the two algorithms it is necessary to consider that a single iteration of the LS algorithm requires on the order of a minute to run in its current implementation on our fastest computer, while an iteration of the GS algorithm requires on the order of a second. Thus, hundreds of GS iterations can be done in the time it takes for a few LS iterations. Possible methods for speeding up the algorithms include taking advantage of the native FFT routines provided on our machines as well as parallelization.

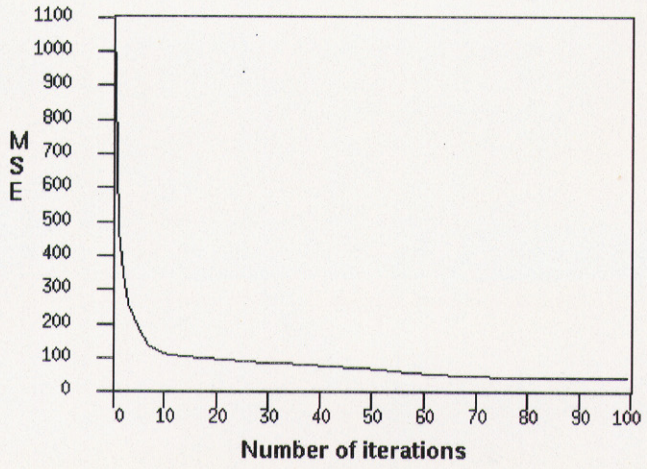

(a)

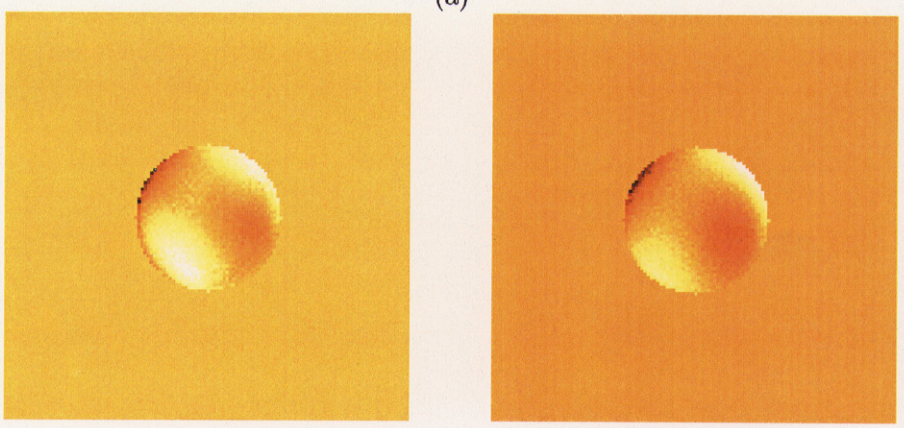

(b) (c)

Figure 6: Mean squared error between estimated and measured image at each iteration is shown in (a). Estimated phase aberrations after 50 and 100 iterations are shown in (b) and (c), respectively.

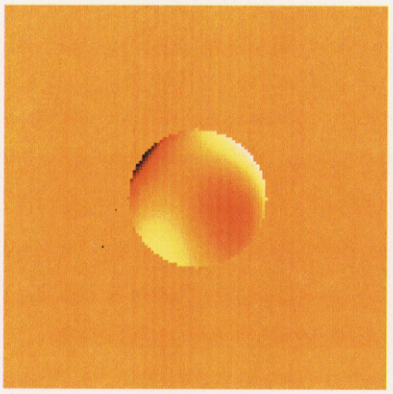

Figure 7: Estimated phase aberration after 4 iterations of the LS algorithm.

For the next simulation, we will demonstrate the effects of undersampling the measured intensity images. This is a situation we expect to encounter with real data, such as with the LIRC II camera on the Lick adaptive optics system. At a wavelength 2.1 microns and a telescope diameter of 3.0 meters, the LIRC II camera has a pixel size of 0.125 arcseconds per pixel, which is 1.7 times larger than what Nyquist requires. Given that information, we will simulate the same phase aberration as before, only this time the detected images will have a pixel size 2.0 times the Nyquist pixel size requirement. Because the phase retrieval algorithms require at least Nyquist sampled data to run properly, we must first upsample the poorly sampled data to Nyquist. The interpolation method appears to have a small, but noticeable effect on the results. For our case, a spline interpolation worked the best. Inputting the upsampled data into the two phase retrieval algorithms, we obtain results as shown in Figure 8 and Table 4. Clearly, the estimated aberrations are not in

Zernike mode number	Actual Coefficient	400 GS Iterations	10 LS Iterations
3	0.30	0.20	0.28
4	0.80	0.71	0.62
5	-0.20	-0.02	-0.14
7	0.50	0.47	0.49
11	0.10	0.13	0.09
all others	0	$\leq$0.11	$\leq$0.08
rms error	0	.3	.2

Table 4: Table of Zernike coefficients for the undersampled data estimated with 400 iterations of the GS algorithm and with 10 iterations of the LS algorithm. Bottom row gives the rms wavefront error in radians for each case.

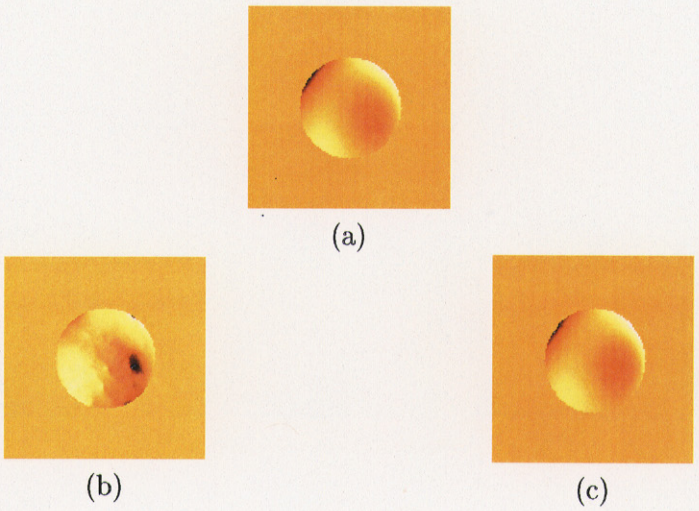

Figure 8: Phase aberration estimation with undersampled data. (a) Actual phase aberration, (b) phase aberration estimated with 400 iterations of the GS algorithms, and (c) phase aberration estimated with 10 iterations of the LS algorithm.

perfect agreement with the actual phase aberrations, as some coefficients are estimated quite accurately and others are not. This makes sense, because if the measured intensity images are not properly sampled, the effects of certain phase aberrations will not necessarily be imaged with the detail fully needed to detect them. Also, various unwanted Zernike modes could be introduced as a result of upsampling the data.

4 Conclusions

Based on the results from the simulations, we can see that phase retrieval can be a useful tool in helping to determine and correct static phase aberrations in adaptive optics systems. Even if the system is undersampled, a great deal of the aberration can still be measured and corrected.

Acknowledgments: We would like to thank Scott Acton of Keck Observatory who provided us with his IDL implementation of least squares phase retrieval, which aided in our understanding and C++ implementation of the algorithm.

References

[1] *R. K. Tyson, Principles of Adaptive Optics, Academic Press, Inc., San Diego, CA, 1991*

[2] *R. W. Gerchberg and W. O. Saxton, Optik* **35**, *237-246 (1972)*

[3] *R. A. Gonsalves, "Phase retrieval and diversity in adaptive optics", Opt. Eng.* **21**, *829-832 (1982)*

[4] *J. R. Fienup, "Phase retrieval algorithms: a comparison", Applied Optics, Vol 21, No. 15, August 1982*

[5] *R. G. Paxman, T. J. Schulz, and J. R. Fienup, "Joint estimation of object and aberrations by using phase diversity", J. Opt. Soc. Am. A/Vol. 9, No. 7, July 1992*

[6] *N. Baba, H. Tomita, and N. Miura, "Iterative reconstruction method in phase-diversity imaging", Applied Optics, Vol. 33, No. 20, July 1994*

[7] *M. G. Lofdahl and G. B. Scharmer, "Wavefront sensing and image restoration from focused and defocused solar images", Astron. Astrophys. Suppl. Ser.* **107**, *243-264 (1994)*

[8] *D. Acton, D. Soltau, and W. Schmidt, "Full-field wavefront measurements with phase diversity", Astron. and Astrophys.,* **309**, *661-672 (1996)*

Technical Information Department • **Lawrence Livermore National Laboratory**
University of California • Livermore, California 94551